Article

Frequency and space-diverse MIMO antenna with enhanced gain

Shilpa Nandedkar,[1*] Shankar Nawale,[2]

[1]*Electronics and Telecommunication Engineering, Maharashtra Institute of Technology, Aurangabad, Maharashtra-431005 India.*
[2]*EC, N B Navale Sinhgad College of Engineering, Solapur, Maharashtra 413255, India.*

ABSTRACT
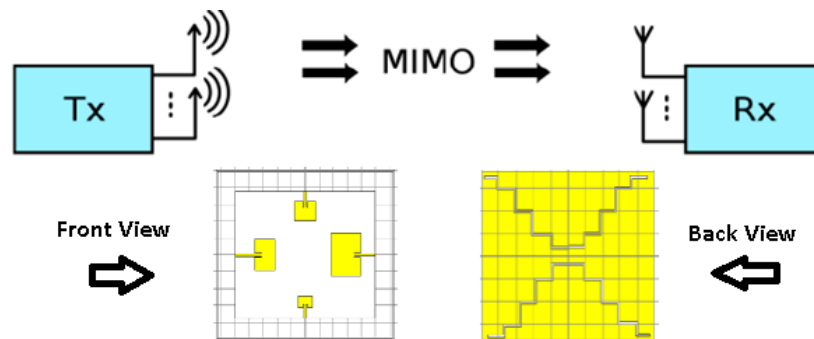
Four-port multiple-input multiple-output (MIMO) antenna with defected ground structure (DGS) is investigated. In this study proposed design performs operations at diverse frequencies (1.8GHz NB-IoT band, 2.4GHz ISM band, 3.1GHz sub 6 GHz, Wi-Max, and 4.8GHz 5G connectivity band). The antenna is excited by a microstrip transmission line. The proposed MIMO antenna occupies a compact area of 20cm*15cm with isolation of less than -15dB among all ports. Radiation characteristics such as return loss and bandwidth are also taken. MIMO performance metrics in terms of Envelop correlation coefficient (ECC), diversity gain (DG), total active reflection coefficient (TARC) and mean effective gain (MEG) are also taken for satisfactory diversity performance.

Keywords: MIMO, DGS, ECC, TARC, MEG, Antenna Design, Mobile Network,

INTRODUCTION

MIMO communication is the need for a non-Line of Sight (LOS) environment in next-generation wireless communication. Diversity techniques can supply, several replicas of the same information signal transmitted over independently fading channels to the receiver. MIMO systems are having implementation challenges that are reviewed in the literature.[1] MIMO antenna with diversity in polarization, frequency, and space is designed and analyzed.[2-8] MIMO antenna offers high gain, superior data rate, range, and reliability without the need for additional bandwidth or power. Multiple antennas with multiple bands having wide bandwidth are needed for next-generation wireless communication systems. The

circularly polarized antenna gives a high gain at 2.4 GHz for WBAN application as mentioned in the literature.[9] MIMO antenna is facing a major problem due to mutual coupling. A lot of investigation was carried out for reducing this coupling between the antenna elements. One of the techniques for mutual coupling reduction is defective ground structure (DGS).[10] DGS provides additional current paths, input impedance, inductance, and capacitance to improve bandwidth. Bandwidth can be improved by changing the length and width of the slots.[11] Parasitic elements are also used with patch antenna which leads to frequency reconfiguration.[12-13] High isolation is achieved by using a metamaterial wall between orthogonally placed planar antenna elements as given in the reference.[14] The decoupling meta material configuration based on the fractal electromagnetic bandgap (EMBG) structure significantly improves the separation between the transmit and receive antenna elements of a densely packed patch antenna array.[15] Different methods have been observed in the survey based on single feed or dual feed, Coplanar waveguide (CPW) feed, using passive components like register, capacitors, and stub/slot/slits resonating structures to create perturbation in the path of the electric field which excites two orthogonal current modes of the same magnitude and quadratic phase difference.[3]

*Corresponding Author: Mrs. Shilpa Nandedkar
Tel: +91-0240-2375250; +91 9423343855
Email: shilpa.nandedkar@mit.asia

Journal of Integrated Science and Technology

J. Integr. Sci. Technol., 2023, 11(2), 482   Pg 1

MIMO configurations described in the literature use different decoupling structures to achieve low mutual coupling between radiating elements such as parasitic elements[17] and meandered lines strips.[18] A MIMO system with a Cylindrical Dielectric Resonator (CDR) antenna gives a dual performance as ultra-wideband and narrowband functionality with a modified feeding structure.[4] DRA structure with MIMO uses out of phase magnetic field which results in increased isolation up to 25 dB within antenna elements as given in the literature.[20] 5G mm-wave application using dual-band quad polarised transmit array[21] shows the higher gain and higher aperture efficiency with polarization diversity. Four parallel-fed monopole elements with Super Wide Band MIMO antennas which gives isolation of 20 dB with metallic barriers between elements were presented in referred literature.[22] fully metallic (seven-layer), circularly polarized Fabry–Perot cavity antenna using laser cutting technology at 300 GHz shows high gain (16.5dB).[23] A MIMO antenna for ISM band application with a significant reduction in mutual coupling (46 dB) and cross-polarization is presented by using a simple string of H-shaped DGS.[24] A quad-port MIMO antenna is reported which has 3.5 GHz (3.4–3.6 GHz) and 4.9 GHz (4.8–5 GHz) frequency bands showing isolation of 16.5 dB.[25] A 5.875 GHz self-decoupled dual-beam MIMO antenna using SIW technology is presented which shows the isolation of 31.65 dB and peak gain of 6.15dB without any decoupling network.[5] Inverted L-shaped strips along with steeped folding strips and neutralization lines promo the cancellation of the coupled induced current between the elements.[6] By parasitic layer with an air gap in 2*2 MIMO antenna using coplanar waveguide feed show 50% reduction in mutual coupling.[28] The Circular Polarization radiation is achieved by embedding three oval slots, in which two of which are deployed at the left and right side of the concentric rings, whereas the third one is deployed at the top section of the concentric rings in two-port MIMO antenna which gives better impedance bandwidth and axial ratio bandwidth.[29] In square patch complementary split-ring resonator and placing a single shorting post close to the antenna center line, higher-order modes of the four-port dual-band MIMO antenna are then suppressed while maintaining satisfactory mutual coupling (<-11 dB) and impedance matching (<-15 dB) performance in the operating band.[30] Depending on the application and required frequency band, different techniques are proposed for improving diversity performance in MIMO antenna. Each method is having advantages as well as limitations. In this study proposed design operates at diverse frequencies (1.8 GHz, 2.4 GHz, 3.1 GHz, 4.8 GHz), excited by a microstrip transmission line.

EXPERIMENT AND RESULTS

Four-port MIMO antenna is designed with four rectangular patch antennas. It is designed with four resonating frequencies such as 1.8 GHz, 2.4 GHz, 3.1 GHz, and 4.8 GHz. The rectangular microstrip patch antenna is the most versatile and commonly used structure in the design of a patch antenna. In this design for substrate glass epoxy material (FR-4) is used which is very cost-effective. It is having a dielectric constant of 4.3 and a thickness of 1.6 mm. The ground plane and conducting patch are made of copper material with a thickness of 0.035 mm. The following design equations are

used for calculating the length and width of the rectangular patch by specifying resonating frequency, dielectric constant, loss tangent, and thickness.[31]

For calculating the width of the patch antenna following equation is used.

$$w = \frac{c}{2f_r}\sqrt{\frac{2}{\varepsilon_r+1}} \qquad (1)$$

w is the width of the patch, C is the velocity of light, ε_r is the dielectric constant, and f_r is resonating frequency.

The length of a patch is calculated by

$$L = L_{eff} - 2\Delta L \qquad (2)$$

L_{eff} is the effective length calculated with the following equation.

$$L_{eff} = \frac{c}{\sqrt{\epsilon_{reff}}\,2f_r} \qquad (3)$$

ΔL is the length extended on both sides and given by the following equation.

$$\frac{\Delta L}{hs} = 0.412\,\frac{(\epsilon_{reff+0.3})\left(\frac{w}{hs}+0.264\right)}{\left((\epsilon_{reff-0.258})\left(\frac{w}{hs}+0.8\right)\right)} \qquad (4)$$

where ϵ_{reff} is the effective dielectric constant given by the following equation.

$$\epsilon_{eff} = \frac{\epsilon_{r+1}}{2} + \frac{\epsilon_{r-1}}{2}\left(\frac{1}{\sqrt{\left(1+\frac{12*hs}{W}\right)}}\right) \qquad (5)$$

where hs is substrate thickness (1.6mm). The length and width of the four patches are shown in the following table.

Table 1 Dimension for four patches with frequency.

Patch No.	Length (mm)	Width (mm)	Frequency (GHz)
1	51.19	40.77	1.8
2	29	38	2.4
3	16.71	29.74	3.1
4	19.19	14.25	4.8

For all patches, inset feed is used. Microstrip line with inset feed is preferred for bandwidth improvement in RMSA.[32] Frequency diversity/switching can also be achieved by adding PIN diodes along with patch elements.[33] Different types of array antenna are also preferred for 5G applications.[34] The ground plane is modified by meandered lines for improving the mutual coupling between ports. The front view and back view of this structure are shown in Figure 1(a) and (b) respectively.

The proposed structure is designed and simulated in CST microwave studio. Radiation parameters such as return loss, bandwidth, impedance, VSWR, directivity, beamwidth, side lobe level, and gain for the individual patch are measured. Pattern diversity is observed between patches 1 and 2 as well as between patches 3 and 4.

Journal of Integrated Science and Technology

J. Integr. Sci. Technol., 2023, 11(2), 482   Pg 2

[a]

[b]
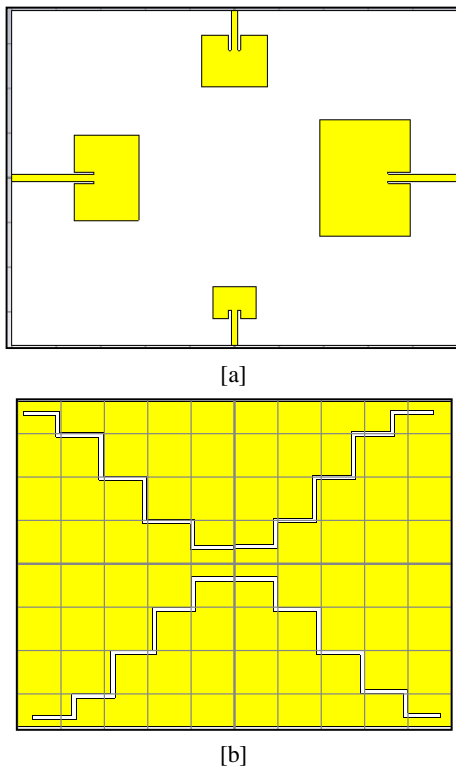
Figure 1. MIMO structure (a) Front view (b) Back view

S PARAMETERS

The scattering parameter (S11) is plotted against frequency which gives return loss for resonating frequency. As shown in Figure 2 for patch1 three resonating frequencies (S11= 2.42, 3.74, and 4.56 GHz) are obtained. It shows return loss as -16.26, -49.26, and -13.01 dB respectively. It gives impedance bandwidth of 130 MHz, 220 MHz, and 360 MHz respectively.
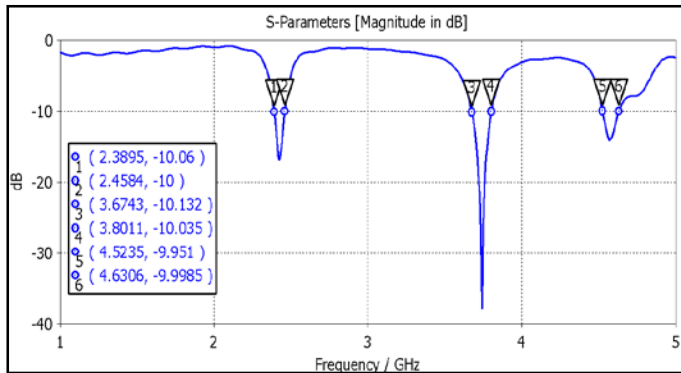
Figure 2. Return loss curve for Patch 1

For patch 2 return loss curve is shown in Figure 3. As shown here it is resonating at 4.8 GHz with a return loss of –20.18 dB. The bandwidth obtained is 270 MHz while the impedance bandwidth is 360 MHz.

For patch 3 return loss curve is shown in Figure 4. It has two resonating frequencies 1.73 and 2.79 GHz. As seen from the graph it has a return loss of -24.53 and -10.67 dB respectively.
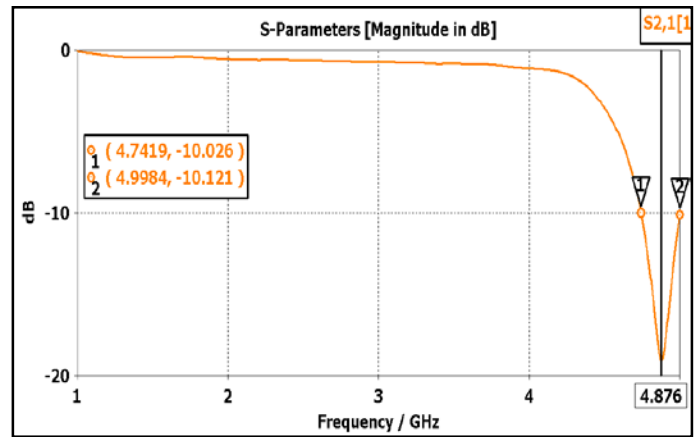
Figure 3. Return loss curve for Patch 2
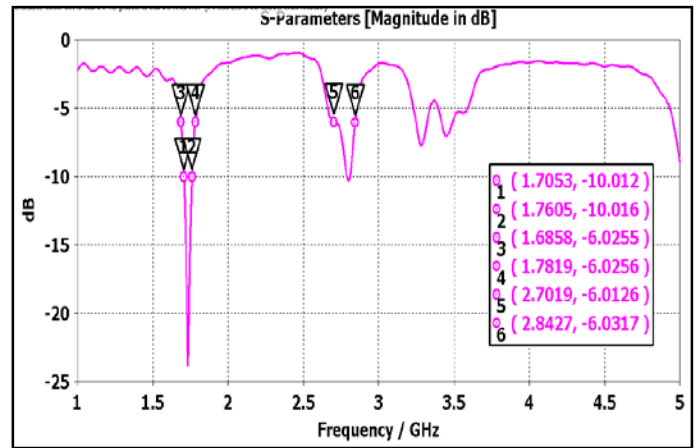
Figure 4. Return loss curve for Patch 3

It has less bandwidth i.e., 60 MHz with impedance bandwidth of 100 and 160 MHz respectively.
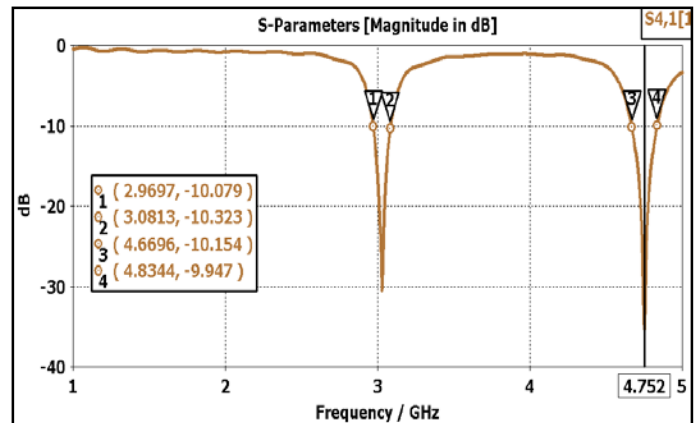
Figure 5. Return Loss curve for Patch 4

For patch 4 return loss curve is shown in Figure 5. It has two resonating frequencies i.e. 3.1 and 4.75 GHz. The figure shows S11 are -26 dB and -40.46 dB respectively. 10 dB bandwidths are 110 and 163 MHz while impedance bandwidths are 192 MHz and 270 MHz respectively. Isolation between ports is plotted concerning frequency.
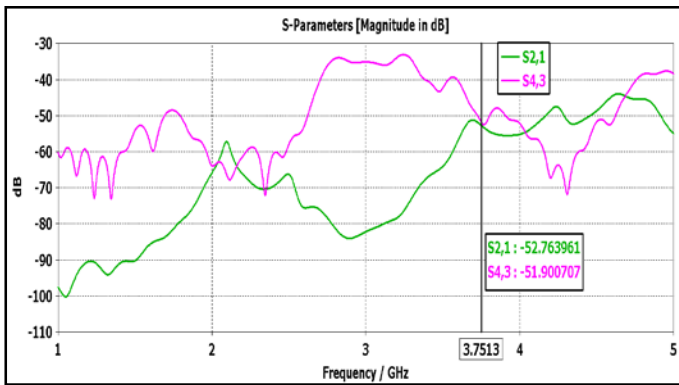
Figure 6. Isolation comparison between ports 1, 2 and 3, 4

Ports 1 and 2 and ports 3 and 4 are having isolation as S21 and S43 as shown in Figure 6. The figure shows S21= -41.19 dB and S43= -50.79 dB respectively at 3.74 GHz.
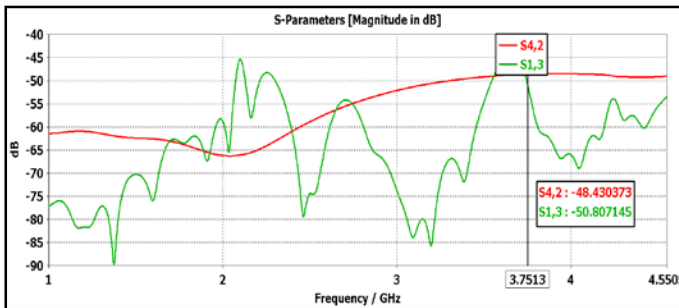
Figure 7. Isolation comparison between ports 1, 3 and 2, 4

Similarly, isolation between ports such as S13 and S42 is shown in Figure 7, which indicates S13= -37.91 and S42 = -48.53 dB respectively.
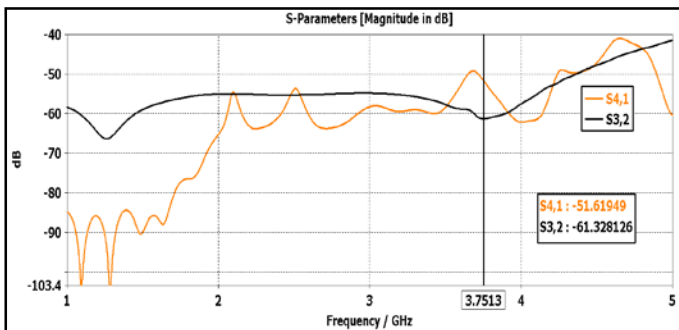
Figure 8. Isolation comparison between ports 1, 4 and 2, 3

As shown in Figure 8, isolation between ports1 and 4 i.e. S41, and between ports 2 and 3 i.e. S32 shows, isolation for the complete frequency range is from -40 to -90 dB.

MIMO PARAMETERS

MIMO parameters such as Envelop Correlation Coefficient (ECC), Diversity Gain (DG), Total Active Reflection Coefficient (TARC), and Mean Effective Gain (MEG) are measured in the following sections.

ECC

The port-to-port correlation between two antennas in a spatial diversity system is defined for receive mode and is calculated in two steps. In the first step radiated far field components are determined (E_θ and E_Φ) for the individual port excitations by considering the transmit mode and keeping all other antenna ports terminated in a matched load. The second step uses statistical angular probability distribution (P_θ and P_Φ) and cross-polar discrimination Z of the incoming wave. The envelope correlation coefficient from radiated fields is obtained by using the following equation. The acceptable value of ECC is less than 0.5.

$$ECC12 = \frac{\left|\iint_{4\pi}^{1}\left[E_1(\theta,\varphi)\times E_2(\theta,\varphi)\right]d\Omega\right|^2}{\iint_{4\pi}^{1}\left|E_1(\theta,\varphi)\right|^2 d\Omega \iint_{4\pi}^{1}\left|E_2(\theta,\varphi)\right|^2 d\Omega} \qquad (6)$$
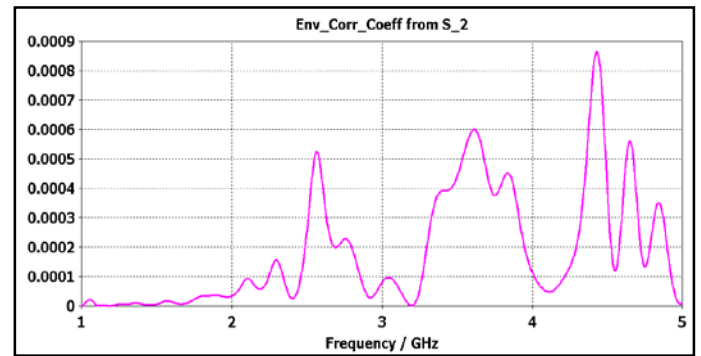
[a]
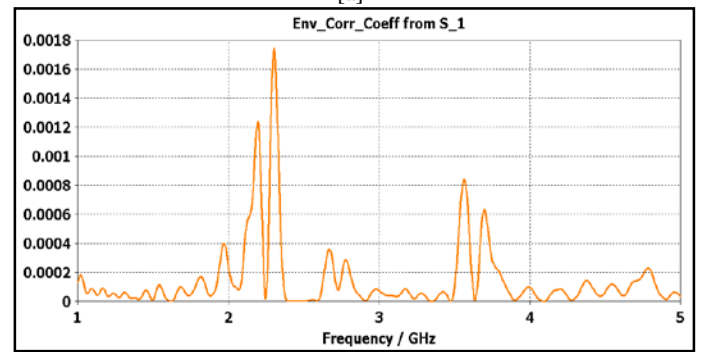
[b]
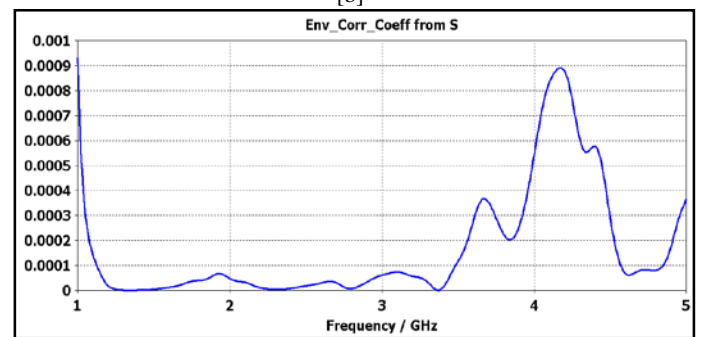
[c]

Figure 9. ECC (a) between ports 1 and 2 (b) between ports 1 and 3 and (c) between ports 1 and 4.

ECC can be calculated either by using S parameters or far-field patterns here it is taken from S parameters as shown in Figure 9. As can be seen from Figure 9 a, b, and c it is well below 0.01.

Journal of Integrated Science and Technology

J. Integr. Sci. Technol., 2023, 11(2), 482   Pg 4

DIVERSITY GAIN

Diversity gain between ports can be obtained by finding the correlation coefficient between branch signals and the signal-to-noise ratio in each branch. It can be calculated from s parameters as well as from far fields. The acceptable value should be 10 dB. It is shown in Figure 10.

As indicated in Figure10 (a) diversity gain between ports 1 and 2 varies from 9.9 to 10 dB in a complete range of 1 to 5 GHz. In ports 1 and 3, it varies from 10 to 9.95 dB as given in Figure 10(b), whereas in ports 1 and 4 as indicated in Figure 10(c) it is from 10 to 9.995 dB. It means it is approaching the ideal value.

Table 2. Comparison of the proposed antenna with the literature

Reference Paper No.	Isolation techniques	Dimensions	Elements	Bands	Gain	ECC
1	Shorting strips	150×150 mm^2	4	699-798 MHz 2.2-2.4 GHz 1.7-2.0 GHz 3.5-4 GHz	2 dBi	<0.1
2	Decoupling network and stubs	117 x 65 x 0.762	6	727–1066 MHz 1.7–1.9 GHz 5.5–5.8 GHz	1.59-9 dBi	0.027
6	T-shaped	30×30×1.6	4	18-27GHz	5.23 dBi	< 0.06
13	Meandered line	116×58×1.6	2	2.45 3.5	1.2 dBi	<0.5
Proposed MIMO	DGS Meandered Line	200x150x1.6	4	2.36-2.48 GHz 3.6-3.8 GHz 4.47-4.81 GHz	9.15dBi	0.01

[a]

[b]

[c]
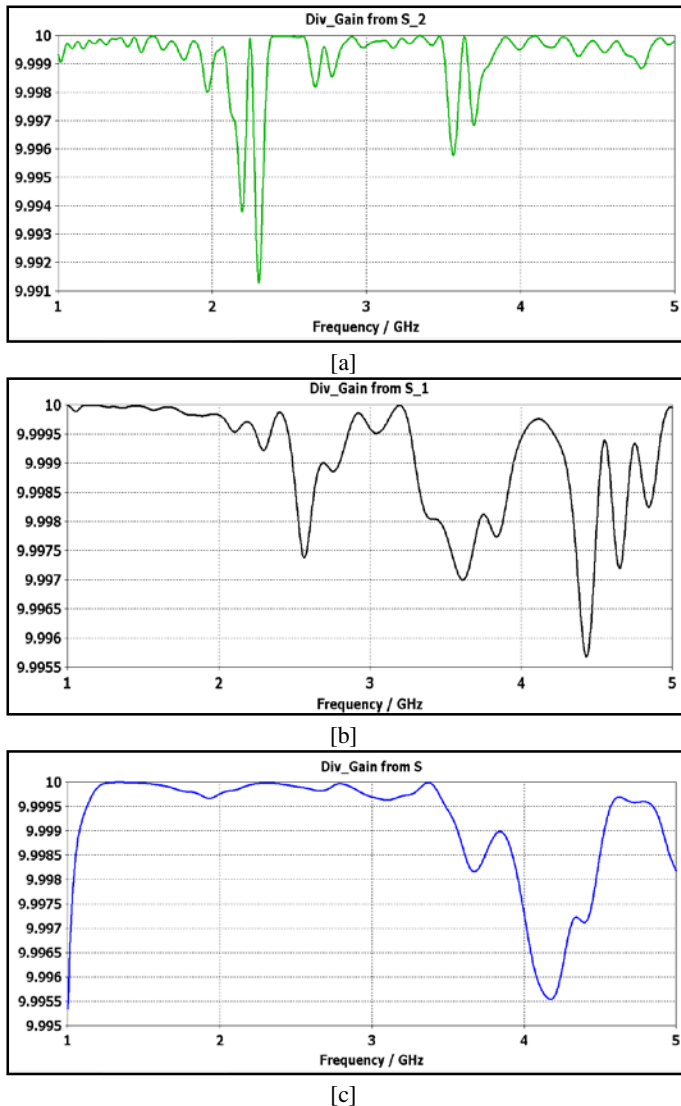
Figure 10. Diversity gain between ports (a) port 1 and 2 (b) port 1 and 3 (c) port 1 and 4

TARC

The total Active Reflection Coefficient (TARC) is a MIMO parameter that determines incident power to the radiated power. It can be calculated from the s parameter with the following equation.[2]

$$\Gamma = \frac{\sqrt{(|S_{ii}+S_{ij}e^{j\theta}|^2)+(|S_{ji}+S_{jj}e^{j\theta}|^2)}}{\sqrt{2}} \qquad (7)$$

Here S_{ij} and S_{jj} are reflection coefficients between ports and S_{ij} and S_{ji} are isolation between ports. Θ is the input feeding phase, where the phase angle is taken 0 degrees. TARC should be less than 10 dB. After calculation, its value is -31.08 dB, which is acceptable.

MEG

Mean effective gain is calculated from S-parameters. It is a measure of how much electromagnetic power it receives in a multipath environment. It is calculated from the following equation.[2]

$$MEG = 0.5\left(1 - \sum_{j=1}^{k}[sij]^2\right) \qquad (8)$$

Where k is a number of antennas, here k is four. MEG is calculated for each port, and it is less than 3 dB which is acceptable. The proposed MIMO antenna is compared with the existing MIMO antenna from the literature in Table 2. It compares isolation enhancement techniques used, dimensions (compactness), number of elements, number of bands obtained, Gain, and ECC.

DISCUSSION

The proposed MIMO antenna is compared with the existing MIMO antenna from the literature in Table 2. It compares isolation enhancement techniques used, dimensions (compactness), number of elements, number of bands obtained, Gain, and ECC. Directivity obtained are 5.52(f=1.8GHz), 7.72 (f=2.4GHz), 7.44(f=3.1GHz), 8.57(f=4.8GHz). VSWR varies from 1.11 to 2.2. Isolation between ports varies from -10 dB to - 50 dB. MIMO parameters such as ECC (0.01), DG (-10dB), TARC (-31dB), MEG (-3dB) are also in

Journal of Integrated Science and Technology

J. Integr. Sci. Technol., 2023, 11(2), 482   Pg 5

acceptable range. From obtained results it is showing enhanced gain of 9.15 dBi which is most preferable for wireless communication.

CONCLUSION

From parametric study, proposed design shows it is applicable for Personal Area Network (PAN) devices operating at 4 different frequencies 1.81 GHz (IoT band), 2.4 GHz (ISM band), 3.1 GHz (Wi-Max), and 4.8GHz (5G connectivity band) with larger directivity up to 8.57dB. At port1 it gives triple band operation. Directivity and gain increases with frequency.

CONFLICT OF INTEREST

The author declared no conflict of interest.

REFERENCES

1. M.S. Sharawi. Printed MIMO Antenna Systems: Performance Metrics, Implementations, and Challenges. *Forum Electromagn. Res. Methods Appl. Technol.* **2014**, 1 (July), 1–11.
2. D. Sharma, B.K. Kanaujia, S. Kumar. Compact multi-standard planar MIMO antenna for IoT/WLAN/Sub-6 GHz/X-band applications. *Wirel. Networks* **2021**, 3.
3. V. Puri, H.S. Singh. Design of an isolation-improved MIMO antenna using a metasurface-based absorber for wireless applications. *Optik (Stuttg).* **2022**, 259, 168963.
4. S.M. Mikki, S. Clauzier, Y.M.M. Antar. Empirical Geometrical Bounds on MIMO Antenna Arrays for Optimum Diversity Gain Performance: An Electromagnetic Design Approach. *IEEE Access* **2018**, 6, 39876–39894.
5. R. Sahoo, D. Vakula. Gain enhancement of conformal wideband antenna with parasitic elements and low-index metamaterial for WiMAX application. *AEU - Int. J. Electron. Commun.* **2019**, 105, 24–35.
6. A. Pandey, J.A. Ansari, I. Masroor, P.K. Mishra. MICROSTRIP LINE-FED BASED QUAD-PORT WIDEBAND MIMO ANTENNA FOR K BAND APPLICATION. **2021**, 6948 (December), 2547–2551.
7. K. Zhi, C. Pan, H. Ren, K. Wang. Statistical CSI-based Design for Reconfigurable Intelligent Surface-aided Massive MIMO Systems with Direct Links. *IEEE Wirel. Commun. Lett.* **2021**, 1–5.
8. H.C. Mora, N.O. G, P.C. T, C.D.E. Almeida. Enabling Signal Space Diversity for MU-MIMO / OFDMA Cellular Systems That Employ Frequency Diversity. *IEEE Access* **2019**, 7, 111204–111221.
9. N.K. Sahu, S.K. Mishra. A compact low SAR and high gain circularly polarized AMC integrated monopole antenna for WBAN applications. *Prog. Electromagn. Res. C* **2021**, 113 (July), 211–226.
10. P. Bharghava, N. Srikanta, P. Muthusamy. MIMO Antenna for UWB with Single Tuned Frequency Notched Characteristics using Parasitic Element Method. *Int. J. Eng. Adv. Technol.* **2019**, 9 (1S5), 14–16.
11. Z. Akhter, R.M. Bilal, A. Shamim. A Dual Mode, Thin and Wideband MIMO Antenna System for Seamless Integration on UAV. *IEEE Open J. Antennas Propag.* **2021**, 2, 991–1000.
12. M. Wagih, G.S. Hilton, A.S. Weddell, S. Beeby. Dual-Polarized Wearable Antenna/Rectenna for Full-Duplex and MIMO Simultaneous Wireless Information and Power Transfer (SWIPT). *IEEE Open J. Antennas Propag.* **2021**, 2, 844–857.
13. V.R. Lad, K. V Kulhalli, J. Kumar. Reconfigurable Sub-6 GHz 5G User-terminal MIMO antenna integrated with ISM 2 . 4 GHz band. **2021**, x, 1–6.
14. P. Das, A.K. Singh, K. Mandal. Metamaterial loaded highly isolated tunable polarisation diversity MIMO antennas for THz applications. *Opt. Quantum Electron.* **2022**, 54 (4), 1–19.
15. M. Alibakhshikenari, B.S. Virdee, C.H. See, et al. Study on isolation improvement between closely-packed patch antenna arrays based on fractal metamaterial electromagnetic bandgap structures. *IET Microwaves, Antennas Propag.* **2018**, 12 (14), 2241–2247.
16. M. Jangid, S. Yadav, M.M. Sharma. A CPW Fed Cross-Shaped Dual-Band Circularly Polarized Monopole Antenna with Strip / Stub / Slot Resonator Loadings. **2022**, 109 (December 2021), 113–123.
17. A. Pandey, N. Nitin, I. Masroor, J.A. Ansari. Gain and bandwidth enhancement with dual-port UWB-MIMO microstrip antenna for satellite communications. **2022**, 2608–2615.
18. A. Moradi, R. Ngah, M. Khalily. Polarized diversity compact planar MIMO antenna for wireless access point applications. *Prog. Electromagn. Res. C* **2019**, 91 (March), 115–127.
19. S. Pahadsingh, S. Sahu. Four port MIMO integrated antenna system with DRA for cognitive radio platforms. *AEU - Int. J. Electron. Commun.* **2018**, 92 (June), 98–110.
20. G.A. Sarkar, S. Ballav, A. Chatterje, S. Ranjit, S.K. Parui. Four-element MIMO DRA with high isolation for WLAN applications. *Prog. Electromagn. Res. Lett.* **2019**, 84 (May), 99–106.
21. L.H. He, Y.L. Ban, G. Wu. Dual-Band Quad-Polarized Transmitarray for 5G mm-Wave Application. *IEEE Access* **2021**, 9, 117520–117526.
22. B.T. Ahmed, D.C. Carreras, E.G. Marin. Design and Implementation of Super Wide Band Triple Band-Notched MIMO Antennas. *Wirel. Pers. Commun.* **2021**, 121 (4), 2757–2778.
23. B. Aqlan, M. Himdi, H. Vettikalladi, L. Le-Coq. A Circularly Polarized Sub-Terahertz Antenna with Low-Profile and High-Gain for 6G Wireless Communication Systems. *IEEE Access* **2021**, 9, 122607–122617.
24. J. Acharjee, K. Mandal, S. Kumar. International Journal of Electronics and Communications (AEÜ) Reduction of mutual coupling and cross-polarization of a MIMO / diversity antenna using a string of H-shaped DGS. *AEUE - Int. J. Electron. Commun.* **2018**, 97, 110–119.
25. J. Huang, G. Dong, J. Cai, H. Li, G. Liu. A quad-port dual-band MIMO antenna array for 5g smartphone applications. *Electron.* **2021**, 10 (5), 1–9.
26. P. Kumari, S. Das. A MIMO Antenna System Using Self-Decoupled EMSIW Dual-Beam Antenna Elements. *IEEE Access* **2022**, 10, 1339–1345.
27. Q. Yang, C. Zhang, Q. Cai, T.H. Loh, G. Liu. A MIMO Antenna with High Gain and Enhanced Isolation for WLAN Applications. *Appl. Sci.* **2022**, 12 (5), 2279.
28. Y.K. Ningsih. Dualband MIMO (2x2) Microstrip Antenna with Co-planar Wave- guide Fed for Long Term Evolution Application. **2021**.
29. J. Kulkarni, C.Y.D. Sim, R.K. Gangwar, J. Anguera. Broadband and Compact Circularly Polarized MIMO Antenna with Concentric Rings and Oval Slots for 5G Application. *IEEE Access* **2022**, 10, 1–1.
30. J.C. Dash, D. Sarkar. A Four-Port CSRR-Loaded Dual-Band MIMO Antenna with Suppressed Higher Order Modes. *IEEE Access* **2022**, 10, 1–1.
31. S.J. Nandedkar, S.D. Nawale. Design and Performance Analysis of Linear Array. *Int. Res. J. Eng. Technol.* **2020**, 07 (04), 33–37.
32. S.H. Yeung, A. Garcia-Lamperez, T.K. Sarkar, M. Salazar-Palma. Comparison of the Performance between a Parasitically Coupled and a Direct Coupled Feed for a Microstrip Antenna Array. *IEEE Trans. Antennas Propag.* **2014**, 62 (5), 2813–2818.
33. K. Dutt, D.S. Sodha. Multiband frequency switchable Microstrip antenna design for satellite application. *J. Integr. Sci. Technol.* **2022**, 10 (3), 189–192.
34. M.K. Pote, P. Mukherji, A. Sonawane. Design of 5G Microstrip patch array antenna for gain enhancement. *J. Integr. Sci. Technol.* **2022**, 10 (3), 198–203.

Journal of Integrated Science and Technology

J. Integr. Sci. Technol., 2023, 11(2), 482   Pg 6